Kovove Mater. 48 2010 227–231
DOI: 10.4149/km_2010_4_227

Microstructure and fracture of TiC-Al_2O_3/W18Cr4V diffusion bonded joint

W. Q. Huang[1,2], Y. J. Li[1]*, J. Wang[1], X. Q. Shen[1]

[1] *Key Laboratory for Liquid-Solid Structural Evolution and Processing of Materials (Ministry of Education), Shandong University, Jinan 250061, Shandong Province, P. R. China*
[2] *College of Mechanical and Electronic Engineering, China University of Petroleum (East China), Dongying 257061, Shandong Province, P. R. China*

Received 18 March 2010, received in revised form 20 May 2010, accepted 25 May 2010

Abstract

Multi-interlayer of Ti/Cu/Ti was used to join TiC-Al_2O_3 composite ceramics with W18Cr4V tool steel. Bonding was performed at 1130 °C for 1 h with a pressure of 15 MPa. The TiC-Al_2O_3/W18Cr4V diffusion bonded joint was examined by means of optical microscope, scanning electron microscope (SEM) and electron probe microanalysis (EPMA). The results indicated that the interfacial transition region was not uniform in thickness. Due to the difference of atom diffusion rate in each substrate, solid-liquid interface migrates at different rates. There were no brittle phases with high hardness in the interfacial transition region. The fracture of a TiC-Al_2O_3/W18Cr4V joint demonstrated a brittle cleavage feature. The interfacial shear strength reached about 141 MPa.

K e y w o r d s: TiC-Al_2O_3/W18Cr4V joint, diffusion bonding, microstructure, fracture

1. Introduction

TiC-Al_2O_3 composite ceramics are widely used in industry as cutting tools and wear resistant coatings because of their high hardness, chemical stability, good strength and toughness at elevated temperatures, and excellent wear resistance [1, 2]. The performance of TiC-Al_2O_3 composite ceramics would be further enhanced if the appropriate technology could be applied to complex shaped components. There has been relatively little experimental work reported about joining TiC-Al_2O_3 composite ceramics to W18Cr4V tool steel.

There are numerous obstacles for successful metal-ceramic joining, the most important of which are the relative inertness of ceramics and the mismatch in coefficient of thermal expansion (CTE). The latter tends to be a major problem when joining dissimilar materials [3]. The mismatch can result in high residual thermal stresses, which originate during cooling from the joining temperature, and consequently form mechanical weak joint [4–7].

In previous study, diffusion bonding of TiC-Al_2O_3 ceramic matrix composites to Q235 low carbon steel and Cr18-Ni8 stainless steel was successfully achieved [8, 9]. In the present work, TiC-Al_2O_3 composite ceramics were bonded to W18Cr4V tool steel using Ti/Cu/Ti multi-interlayer as the stress relief interlayer. The microstructure and element distribution near the interface of TiC-Al_2O_3/W18Cr4V was analysed. Microhardness and shear strength of the diffusion-bonded joint was measured. In addition, the shear fracture morphology was observed and the compositions in the fractured face were measured. This work provides an experimental basis for improving the performance of the TiC-Al_2O_3/W18Cr4V diffusion bonded joint.

2. Materials and experiments

2.1. Experimental materials

The materials used in the present work were TiC-Al_2O_3 composite ceramics and W18Cr4V tool steel. TiC-Al_2O_3 composite ceramics were made by hot

*Corresponding author: tel.: +86 0531 88392924; fax: +86 0531 82609496; e-mail address: yajli@sdu.edu.cn

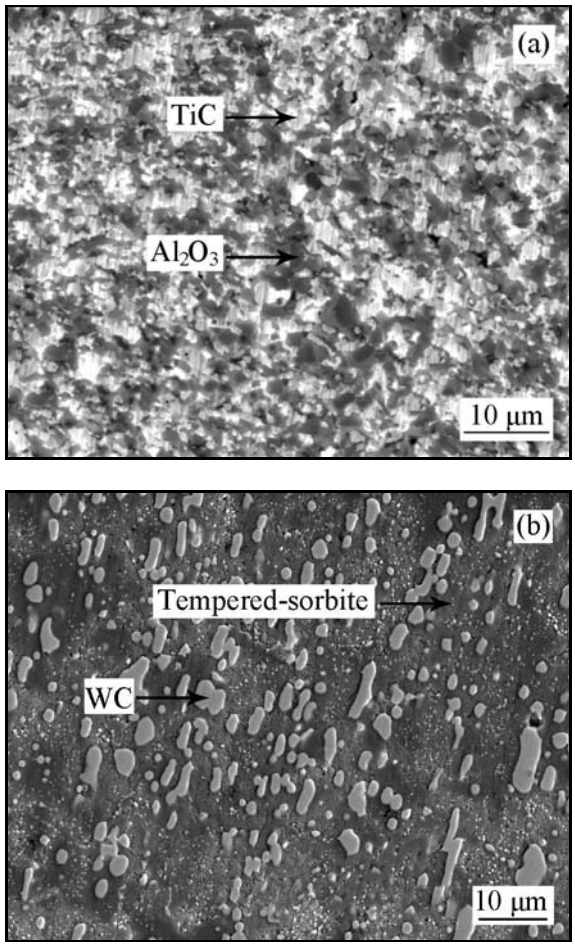

Fig. 1. Microstructure of parent materials: (a) TiC-Al_2O_3 composite ceramics, (b) W18Cr4V.

pressure sintering (HPS) to a final circle plate having dimension ø 52 × 3.5 mm^2. TiC-Al_2O_3 composite ceramics consist of Al_2O_3 matrix and TiC particles. The chemical composition of TiC-Al_2O_3 is 65.6 Al_2O_3 and 34.4 TiC (wt.%). The size of W18Cr4V circle plate specimen is ø 52 × 2 mm^2. The microstructures of TiC-Al_2O_3 composite ceramics and W18Cr4V tool steel are shown in Fig. 1. The dark TiC particles are dispersed in the white alumina matrix (Fig. 1a). As shown in Fig. 1b, the dark matrix is the tempered-sorbite, and discontinuous grey phases are carbides mainly containing W. Multi-interlayer of Ti/Cu/Ti at 60 μm thickness was employed as the thermal stress relief interlayer.

2.2. Experimental procedure

Before diffusion bonding, the surfaces to be joined were ground with abrasive paper, and cleaned by immersing in acetone. After that, the test plates were overlapped and placed into a vacuum chamber. Technological parameters used in the test were: the heating temperature $T = 1130$ ℃, the pressure $P = 15$ MPa,

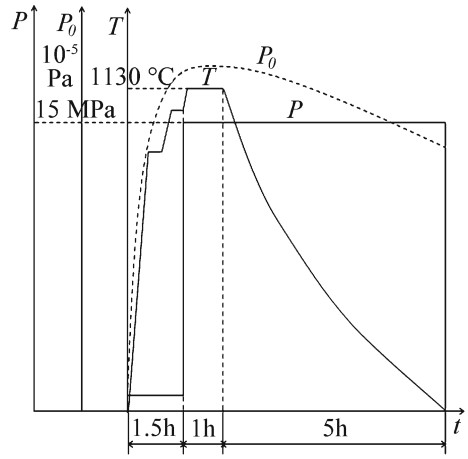

Fig. 2. Technological parameters during diffusion bonding of TiC-Al_2O_3 with W18Cr4V.

the holding time $t = 1$ h and the vacuum degree 10^{-5} Pa. The parameter cycle during diffusion bonding is shown in Fig. 2. The cooling process was conducted in a vacuum chamber that was cooled by circuit water. When the chamber temperature was cooled to 100 ℃, the TiC-Al_2O_3/W18Cr4V diffusion bonded joints were taken out from the chamber.

2.3. Experimental methods

A series of specimens were cut from the TiC-Al_2O_3/W18Cr4V diffusion bonded joint region with a lining cutting machine and were prepared into metallographic specimens by grinding and polishing. Finally, these specimens were etched with a mixed solution consisting of 95 % nitric acid and 5 % alcohol for 10 s.

Microstructure characteristics near the TiC-Al_2O_3/W18Cr4V interface were observed by an optical microscope (OM) and JXA-840 scanning electron microscope (SEM). The microhardness distribution near the TiC-Al_2O_3/W18Cr4V interface was measured by SHIMADZU microsclerometer, with a test load of 100 g for 10 s. The interfacial shear strength was measured using a WEW-600E test machine at a shearing speed of 0.2 mm min^{-1}. The fracture morphology was observed and the compositions on the fractured face were analysed by JXA-8800R electron probe microanalysis (EPMA).

3. Results and analysis

3.1. Microstructure

The microstructure characteristics and element distribution of the TiC-Al_2O_3/W18Cr4V diffusion bonded joint are shown in Fig. 3. It is observed

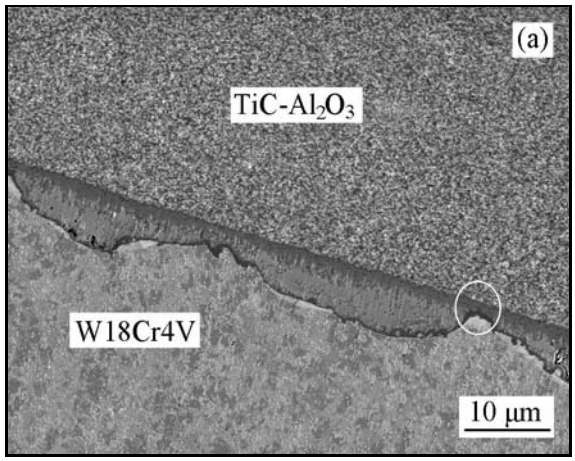

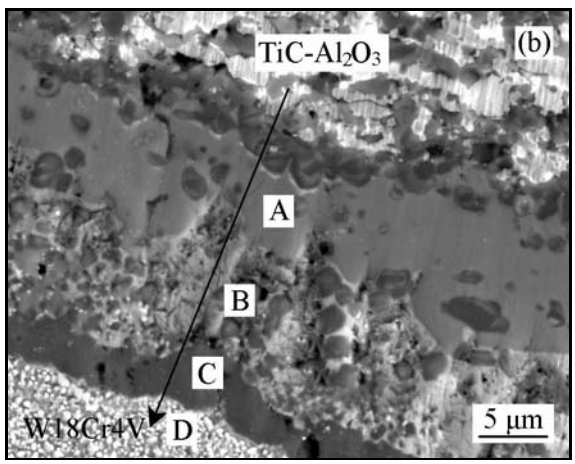

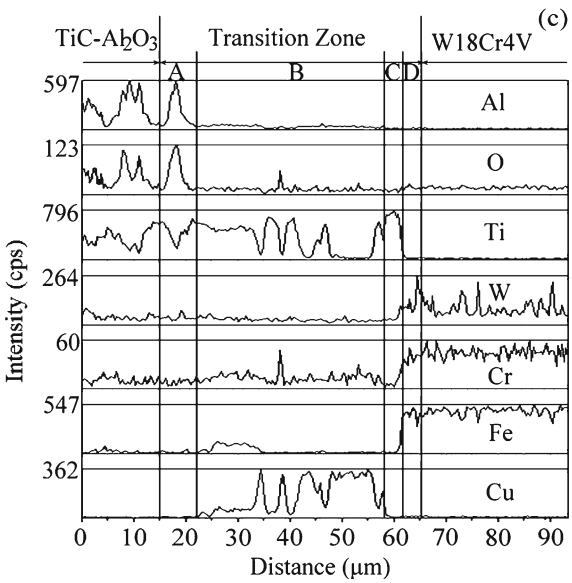

Fig. 3. Microstructure characteristics and element distribution near the TiC-Al_2O_3/W18Cr4V interface: (a) lower magnification, (b) higher magnification, (c) element distribution (scanned location shown in Fig. 4b).

that the Ti/Cu/Ti multi-interlayer was well combined with the two substrates: TiC-Al_2O_3 and W18Cr4V. The interface seems to be continuous and free of defects. Figure 3a illustrates that the interface between the diffusion transition region and TiC-Al_2O_3 is flat and straight; however, the interface is zigzag on the W18Cr4V side. Similar interfacial morphology was also observed in other samples, the technological parameters of which are the same as mentioned above. The interfacial transition region is not uniform in thickness. Due to the difference of atom diffusion rate in each substrate, solid-liquid interface migrates at different rates.

As shown in Fig. 3b, the various microstructure morphologies were formed due to the diffusion and metallurgic reaction of the atoms at the TiC-Al_2O_3/W18Cr4V interface. These microstructures were recognized and labelled, starting from the TiC-Al_2O_3/Ti interface and moving to the underside, that is, into the Ti/Cu/Ti and the Ti/W18Cr4V interface. Region A is a deep grey region close to the TiC-Al_2O_3, region B is a relatively wide non-homogeneous region, region C is a narrow black ribbon region and region D is a white granular region close to the W18Cr4V.

The element distribution near the TiC-Al_2O_3/W18Cr4V interface was measured by EPMA. The test parameters are: working voltage 20 kV and working current 2.5×10^{-5} mA. Line scans were conducted perpendicular to the interface; measured location was shown in Fig. 3b. The element distribution near the interface was shown in Fig. 3c. It indicated that: (1) region A mainly contained Al and Ti, among which the Al content changed greatly and having more Ti; (2) region B mainly contained Cu, Ti and a small quantity of W, Cr, Fe; (3) region C and D contained Ti, Fe and W, and a small quantity of Cr. This indicated that the forming of microstructures in the transition region attributed to the diffusion reaction between Ti and Cu in the Ti/Cu/Ti multi-interlayer, or between Ti, Cu and Al from TiC-Al_2O_3. However, only a small amount of W, Cr and Fe diffused into the transition region, and the diffused W mostly accumulated at the interface close to W18Cr4V.

3.2. Microhardness

In order to evaluate the effect of microstructure morphology at the interface on the properties of the joint, the microhardness distribution was measured from W18Cr4V, moving to the interfacial transition region and TiC-Al_2O_3, as shown in Fig. 4.

The microhardness test results indicated that the microhardness near the interfacial transition region on the W18Cr4V side was only slightly higher than that on the steel side, and on the TiC-Al_2O_3 side, it was obviously lower than that of the ceramic substrate. It indicated that no brittle phases with higher hardness were formed in the interfacial transition region.

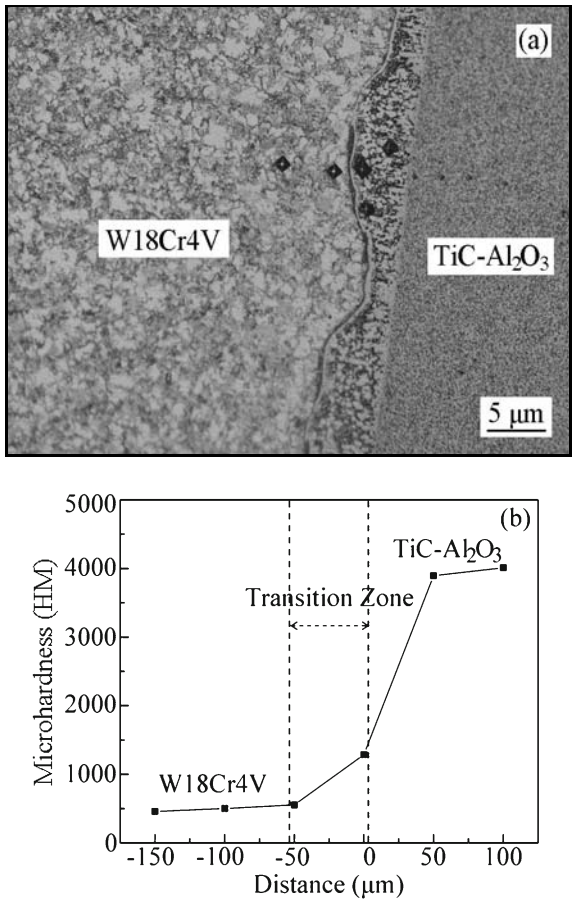

Fig. 4. Microhardness distribution near the TiC-Al_2O_3/W18Cr4V interface: (a) measured location, (b) microhardness distribution.

This is beneficial in improving the properties of joint.

3.3. Shear strength and fracture characterization

In order to explore the mechanical property of TiC-Al_2O_3/W18Cr4V diffusion bonded joint, joint strength was quantified by means of shear strength testing. The relationship between pressure and displacement in shear strength measurement is shown in Fig. 5. When the maximum pressure was 14.1 kN, the diffusion-bonded joint was destroyed. The shear area of the specimen measured 100 mm^2. So the maximum pressure, 14.1 kN, divided by the shear area, 100 mm^2, resulted in shear strength of 141 MPa. The high shear strength mainly attributed to the following aspects: Ti/Cu/Ti multi-interlayer lowered the residual stress generated between TiC-Al_2O_3 and W18Cr4V due to the mismatch in CTE. The interdiffusion of elements occurred, reaction layers and good metallurgical combination formed at the interface. Metals in the interlayer flowed into voids existing in the ceramics, thus, plasticity and mechanical coherence were formed [10].

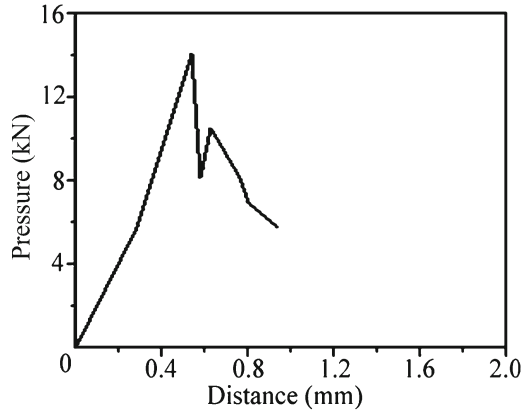

Fig. 5. The relationship between pressure and displacement in shear measurement.

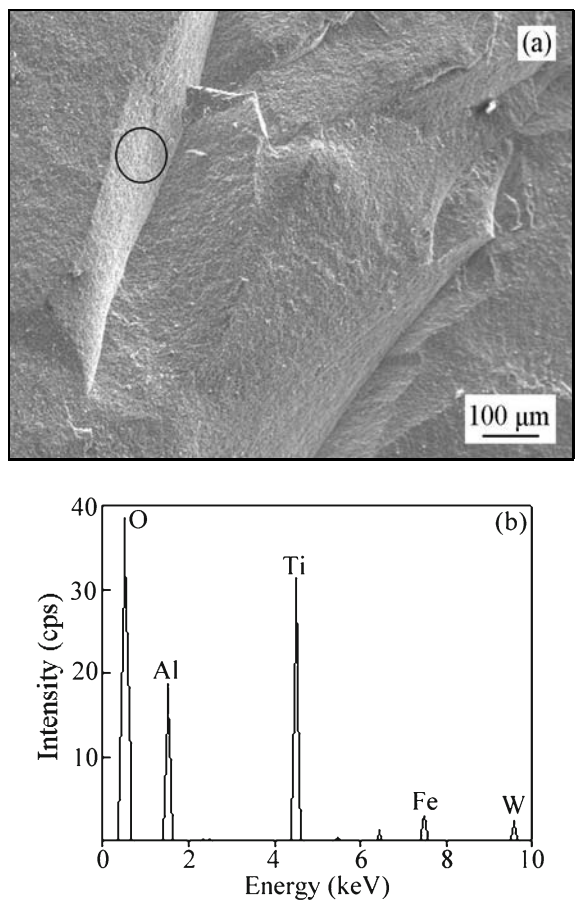

Fig. 6. Fracture morphology and EPMA analysis of TiC-Al_2O_3/W18Cr4V joint: (a) fracture morphology, (b) EPMA analysis.

The fracture morphology of TiC-Al_2O_3/W18Cr4V joint is shown in Fig. 6a. The fracture reveals brittle cleavage features. There are typical cleavage steps on the fracture surface. Fracture colour is consistent with that of TiC-Al_2O_3 composite ceramics. EPMA ana-

lysis (the probe voltage: 4.9 keV, scanned location labelled with white circle shown in Fig. 6a) of the fracture surface demonstrated strong peaks of Al, O and Ti, and very weak peaks of Fe and W (Fig. 6b).

Observation and analysis of the fracture morphology, combined with results of composition analysis for the fracture surface, show that the fracture location is on the TiC-Al_2O_3 side of the bonded joint. The results demonstrate the potential for forming a strong joint.

4. Conclusions

1. Ti/Cu/Ti multi-interlayer was used to join TiC--Al_2O_3 composite ceramics with W18Cr4V tool steel. Bonding was performed at 1130 ℃ for 1 h with a pressure of 15 MPa. The interfacial shear strength reached about 141 MPa.

2. The interface is flat and straight on the TiC--Al_2O_3 side and zigzag on the W18Cr4V side. The transition region was not uniform in thickness. In the transition region, Al, Ti and Cu diffused greatly, and only a small amount of W, Cr and Fe diffused into the transition region.

3. The test results of microhardness indicated that there were no brittle phases with high hardness in the interfacial transition region. The fracture of TiC--Al_2O_3/W18Cr4V diffusion bonded interface demonstrated brittle cleavage fracture features. Fracture occurred on the TiC-Al_2O_3 side of the bonded joint.

Acknowledgements

This project was sponsored by the National Natural Science Foundation of China (50874069), the Ph.D. Programs Foundation of Ministry of Education of China (200804220020), Development Project of Science and Technology of Shandong Province (2007GG10004016), Shandong Province Natural Science Foundation (Y2007F54) and Excellent Mid-Youth Foundation of Shandong Province (2006BS04004).

References

[1] DENG, J. X.—CAN, T. K.—SUN, J. L.: Ceram. Int., *31*, 2005, p. 249. doi:10.1016/j.ceramint.2004.05.009
[2] ATONG, D.—CLARK, D. E.: Ceram. Int., *30*, 2004, p. 1909.
[3] JADOON, A. K.—RALPH, B.—HORNSBY, P. R.: J. Mater. Process. Tech., *152*, 2004, p. 257. doi:10.1016/j.jmatprotec.2003.10.005
[4] MARTINELLI, A. E.—DREW, R. A. L.: Mater. Sci. Eng., *191 A*, 1995, p. 239.
[5] KLIAUGA, A. M.—TRAVESSA, D.—FERRANTE, M.: Mater. Charact., *46*, 2001, p. 65. doi:10.1016/S1044-5803(00)00095-4
[6] MARKS, R. A.—SUGAR, J. D.—GLAESER, A. M.: J. Mater. Sci., *36*, 2001, p. 5609. doi:10.1023/A:1012565600601
[7] SUGANUMA, K.—MIYAMOTO, Y.—KOIZUMI, M.: Ann. Rev. Mater. Sci., *18*, 1988, p. 47.
[8] HUANG, W. Q.—LI, Y. J.—WANG, J.: Kovove Mater., *48*, 2010, p. 173.
[9] HUANG, W. Q.—LI, Y. J.—WANG, J.—JIANG, Q. L.: Kovove Mater., *48*, 2010, p. 271.
[10] JI, X. Q.—LI, S. J.—MA, T. Y.: J. Chn. Ceram. Soc., *30*, 2002, p. 305.